Corrosion Science 121 (2017) 126–132

Contents lists available at ScienceDirect

Corrosion Science

journal homepage: www.elsevier.com/locate/corsci

Sulphidation of Au-Ag alloys in the presence of pyrite (experimental data)

Galina Palyanova*, Konstantin Kokh, Yurii Seryotkin

Sobolev Institute of Geology and Mineralogy, Novosibirsk State University, Novosibirsk, Russia

ARTICLE INFO

Keywords:
A. Alloy
A. Silver
B. EPMA
B. X-ray diffraction
C. Sulphidation

ABSTRACT

Dry annealing of Au-Ag alloys (Au, $Au_{0.56}Ag_{0.44}$, $Au_{0.35}Ag_{0.65}$, $Au_{0.19}Ag_{0.81}$ and Ag), together with pyrite as a source of sulphur, at 450 °C was used to study the mechanisms of corrosion and transition of metal forms of noble metals to sulphide forms. In the experiment with Ag plates the silver completely sulphidates to form acanthite Ag_2S and pyrite desulphidates to form pyrrhotite $Fe_{1-y}S$. In the experiments with the Au-Ag plates there also formation of an uytenbogaardtite phase and ennobling of Au-Ag alloys take place. Gold in the absence of silver stabilizes pyrite and prevents its transition to pyrrhotite.

1. Introduction

Pyrite is one of the host minerals accumulating gold and silver in many of the world's gold deposits [1–3]. Pyrite is frequently intergrown with native gold or contains its microinclusions [4–7]. At some deposits, pyrite along with native gold contain microinclusions of Au-Ag sulphides – acanthite (Ag_2S), uytenbogaardtite (Ag_3AuS_2) and petrovskaite (AgAuS) [8–10]. A number of deposits are characterized by the development of dark rims of Au-Ag sulphides after native gold and silver [11]. Study of natural samples showed that the composition of these rims depends on the fineness of native gold after which they form: uytenbogaardtite forms after gold of fineness above 380‰, whereas petrovskaite, above 650‰. At high temperatures, gold and silver do not virtually dissolve in the iron-sulphide melt, and on cooling and quenched annealing crystallize to form Au-Ag alloys and Au-Ag sulphides [12,13]. Tarnishing of jewelry productions of gold and silver or the appearance of a dark film on Au-Ag alloys are attributed to silver sulphide. In our experiments Au-Ag alloys have turned black due to sulphidation, but we found acanthite, uytenbogaardtite and Au-enriched noble alloys [11]. The sulphidation mechanism of native gold and source of sulphur for the occurrence of sulphidation reactions of noble metals in natural processes is unclear. It is assumed that this might be native sulphur, sulphides of nonferrous metals or gaseous sulphur [14–18]. At many gold deposits that contain native gold and sulphides of nonferrous metals, acanthite (Ag_2S), uytenbogaardtite (Ag_3AuS_2) or petrovskaite (AgAuS) were not found, which may be due to the difficulty of detecting them because of their microscopic sizes and low hardness. In many ores, these and other chalcogenides cause severe processing problems and loss of gold. Some gold ores that contain pyrrhotite are more troublesome than others, depending on the type of pyrrhotite present [5].

The aim of this work is to study the mechanisms of corrosion and transformation of metal forms of noble metals into sulphide form in the presence of pyrite, which is a potential source of sulphur in natural ore-forming processes. One of the tasks of the study is to reveal the influence of silver and gold on the transition of pyrite to pyrrhotite on heating and to determine the compositions of formed Au-Ag sulphides. Knowledge of all mineral forms of the occurrence of noble metals, especially those that are hard to detect in sulphide ores is very important and is of interest to mineralogists, technologists and metallurgists.

2. Experiments and analytical methods

2.1. Starting compositions

The experiments on solid-phase diffusion [19] have been conducted using Au-Ag alloys of varying composition and pyrite single crystal from the Berezovskoe gold-quartz deposit (Ural, Russia). Microprobe analysis showed that the pyrite crystal was homogeneous and did not contain micro impurities. First, a ~5–6 mm thick plate was cut from the crystal. Gold-silver alloys of $Au_{0.19}Ag_{0.81}$, $Au_{0.35}Ag_{0.65}$ and $Au_{0.56}Ag_{0.44}$ composition were synthesized from a stoichiometric mixture of metals and were rolled out to the thickness of ~200 μm and cut into plates measuring 3 × 3 mm. Also pure silver and gold plates 300 and 100 μm in thickness were used. Unlike the earlier performed experiments at 500 °C [17], in which pyrite blocks and plates of Au-Ag alloys were placed successively, as puff pastry, into one big long ampoule, in new experiments one Au-Ag plate was put between the pyrite blocks, the other was isolated by a quartz column

* Corresponding author.
E-mail address: palyan@igm.nsc.ru (G. Palyanova).

http://dx.doi.org/10.1016/j.corsci.2017.03.020
Received 25 January 2017; Received in revised form 22 March 2017; Accepted 23 March 2017
Available online 25 March 2017
0010-938X/

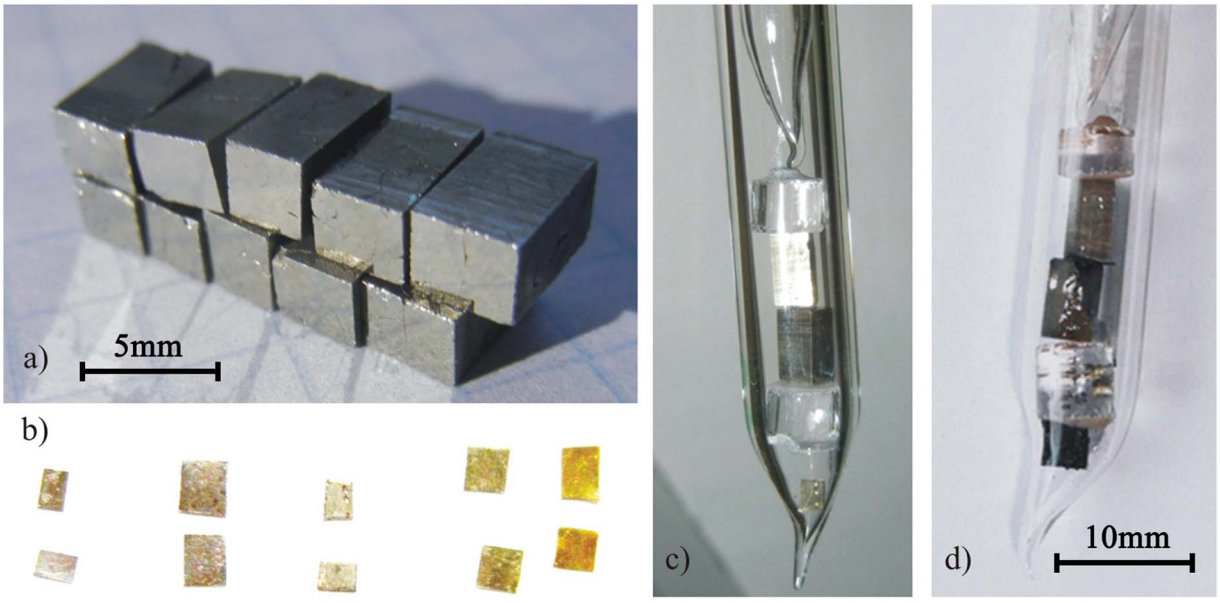

Fig 1. Pyrite blocks (a) and Au-Ag plates of varying composition (b), and the ampoule with Au-Ag plates of composition $Au_{0.19}Ag_{0.81}$ before (c) and after the experiment (d).

Table 1
Chemical compositions of solid-phase products formed at the contact of pure gold, Au-Ag alloys and pure silver plates with pyrite blocks at 450 °C.

№	Starting composition	Compositions of new solid phases (formula)		
		Au-Ag alloys[a]	Ac[a] Uyt[a]	Pyrrhotite $Fe_{1-y}S/FeS_x$(n[b])
1	$Au < < FeS_2$	–	–	–
2	$Au_{0.56}Ag_{0.44} < < FeS_2$	$Au_{0.60\text{-}0.62}Ag_{0.40\text{-}0.38}$	$Ag_{2.02\text{-}1.97}S_{0.98\text{-}1.03} > > Ag_{3.64\text{-}3.20}Au_{0.24\text{-}0.44}S_{2.12\text{-}2.36}$	$Fe_{0.860 \pm 0.002}S/FeS_{1.163}$ (4)
3	$Au_{0.35}Ag_{0.65} < < FeS_2$	$Au_{0.43\text{-}0.47}Ag_{0.57\text{-}0.53}$	$Ag_{2.29\text{-}2.19}S_{0.71\text{-}0.81} > > Ag_{3.55\text{-}3.30}Au_{0.34\text{-}0.44}S_{2.11\text{-}2.28}$	$Fe_{0.873 \pm 0.002}S/FeS_{1.145}$ (5)
4	$Au_{0.19}Ag_{0.81} < < FeS_2$	$Au_{0.47\text{-}0.52}Ag_{0.53\text{-}0.48}$	$Ag_{2.11\text{-}1.96}S_{0.89\text{-}1.04} > > Ag_{3.57\text{-}3.48}Au_{0.29\text{-}0.46}S_{2.14\text{-}2.06}$	$Fe_{0.866 \pm 0.002}S/FeS_{1.155}$ (4)
5	$Ag < < FeS_2$	–	$Ag_{1.96\text{-}1.86}S_{1.04\text{-}1.14}$	$Fe_{0.867 \pm 0.002}S/FeS_{1.153}$ (4)

[a] Calculations for Au-Ag alloys for 1, acanthite for 3 and uytenbogaardtite for 6 formula units.
[b] n – number of analyses.

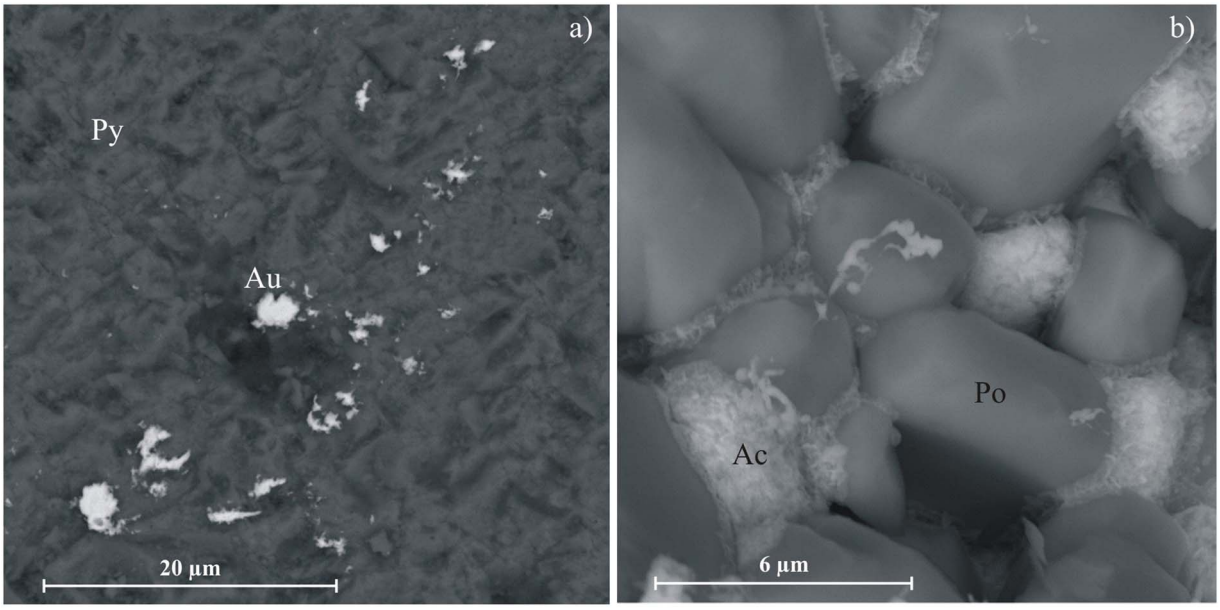

Fig. 2. SEM photo of the surface of pyrite blocks after experiments: (a) with fine-dispersed gold particles (experiment with starting composition Au + FeS_2 (No. 1, Table 1)), (b) with silver sulphide and pyrrhotite (experiment with starting composition Ag + FeS_2 (No. 5, Table 1)).

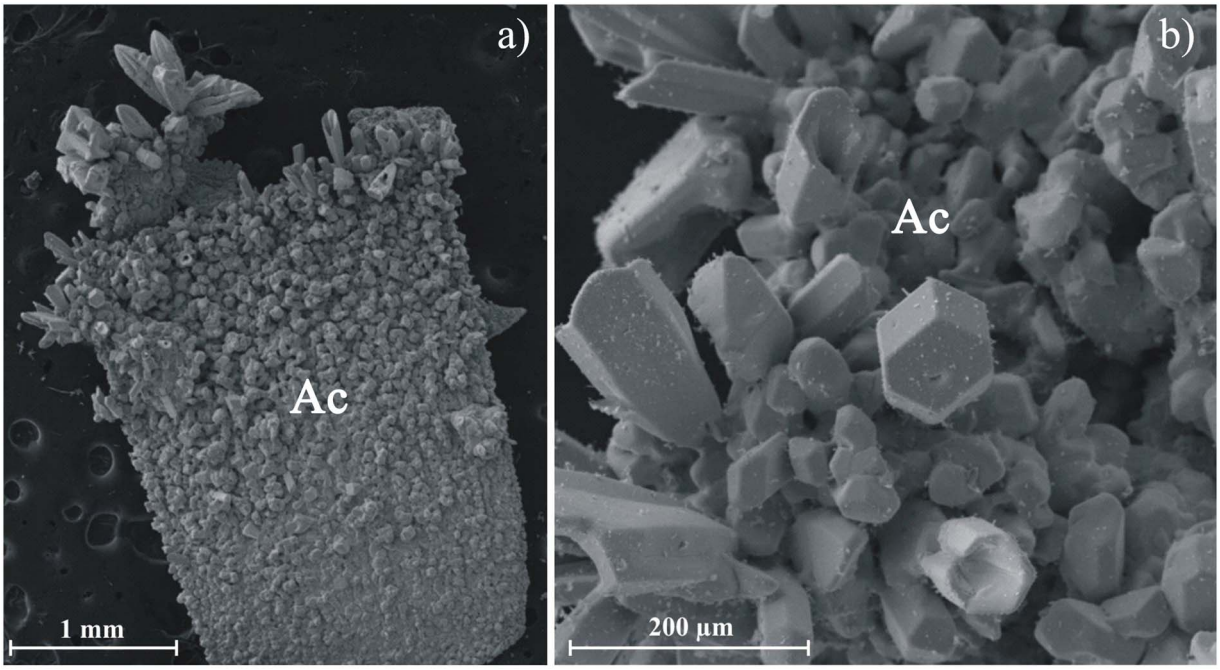

Fig. 3. Crystals of silver sulphide (acanthite, Ac) grown on the silver plate that was out of contact with pyrite (experiment No. 5, Table 1): a – SEM photo of the plate, b – SEM photo of crystals.

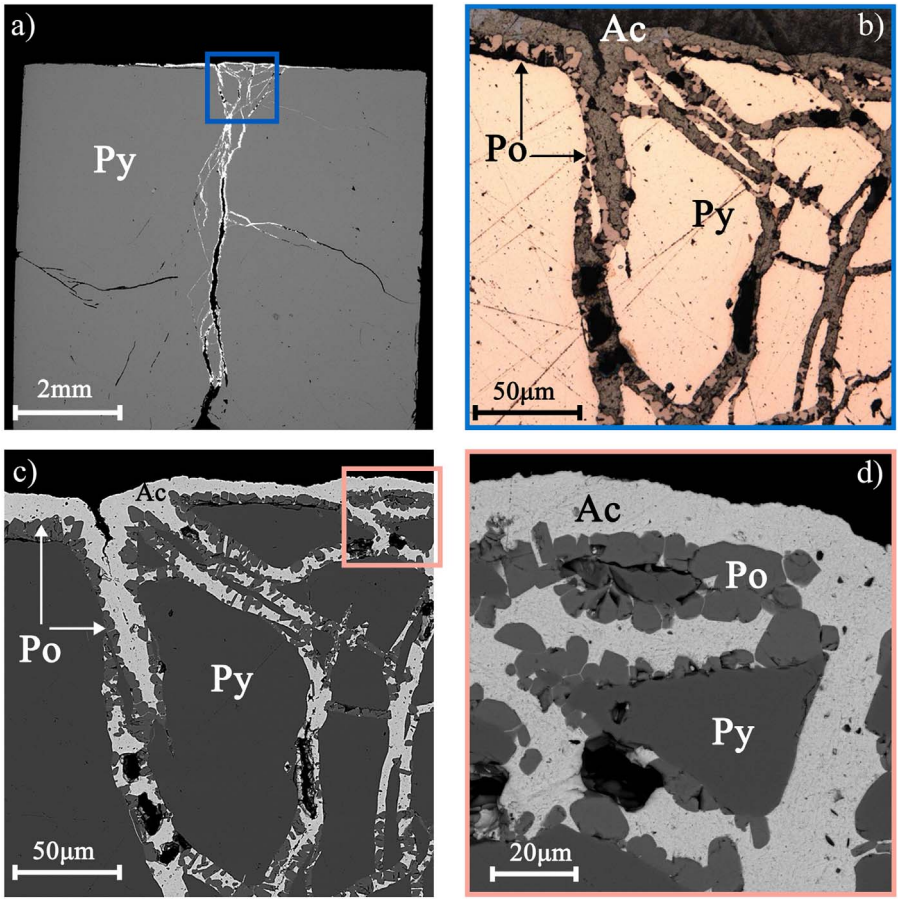

Fig. 4. SEM (a,c,d) and optical photo (b) of the longitudinal section of pyrite block fragments after the experiment with the starting composition Ag + FeS_2 (No. 5, Table 1) – with newly formed solid phases: a – c – acanthite with pyrrhotite on the surface and in cracks of pyrite, d – fragments of pyrite grains with overgrown crystals of pyrrhotite and acanthite.

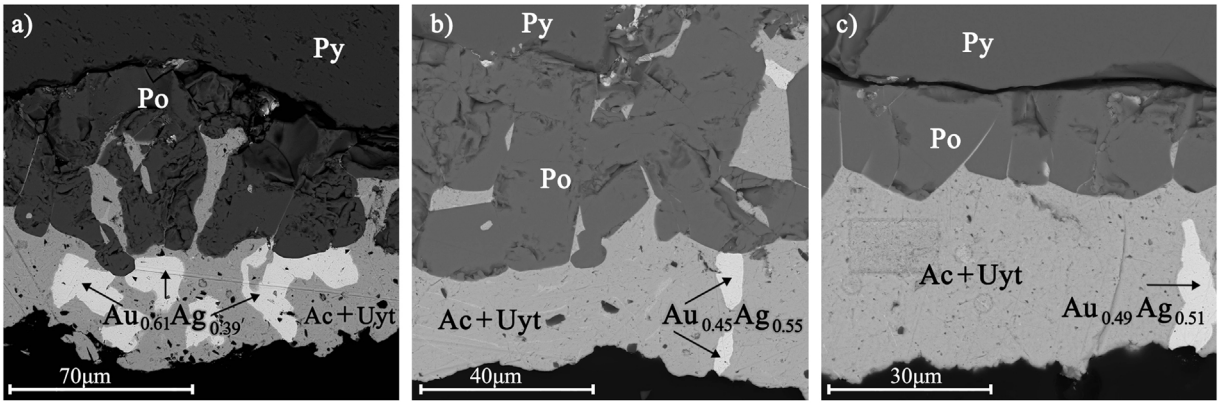

Fig. 5. SEM photo of phases in the reaction zone formed at the contact of pyrite and Au-Ag alloys of initial compositions $Au_{0.56}Ag_{0.44}$ (a), $Au_{0.35}Ag_{0.65}$ (b) and $Au_{0.19}Ag_{0.81}$ (c). Symbols of phases: Py – pyrite, Po – pyrrhotite, Ac – acanthite, Uyt – uytenbogaardtite, $Au_{1-z}Ag_z$ – compositions of newly formed Au-Ag alloys.

from pyrite and each of these sets of starting substances was placed separately into a short quartz ampoule 5 mm in diameter.

After packing, all ampoules were sealed under 10^{-3}torr, slowly heated to 450 °C in the isothermal zone of the furnace, and kept at this temperature for 39 days. After annealing, the ampoules were cooled to room temperature in the switched off furnace. Fig. 1 shows, as an example, the starting substances – pyrite blocks (a) and Au-Ag plates of various composition (b), and one of the ampoules before (c) and after the experiment (d).

2.2. Analytical techniques

Optical microscopy, scanning electron microscopy (SEM), electron microprobe analysis (EPMA) and X-ray powder diffraction methods were applied to study the samples. A polished section was prepared from synthesized phases for microscopy analyses. Studies on the chemical composition of the synthesized substances were carried out using MIRA 3 LMU SEM (TESCAN Ltd.) combined with the micro-analysis system INCA Energy 450+ on the basis of the high sensitive silicon drift detector XMax-80, and WDS INCA Wave 500 (Oxford Instruments Ltd.) (Analytical Center for Multielemental and Isotope Research, Novosibirsk, Russia). Operation conditions: accelerating voltage, 20 kV; probe current, 1.5 nA; spectrum recording, 15 s; and spot size, 12 μm. In all measurements, the electron beam was slightly defocused for reducing the effect of a sample micro relief and decreasing the destructive influence of the electron beam on unstable Au-Ag sulphides. Pure silver, gold and PbS and $CuFeS_2$ were used as standards for Ag, Au, S, and Fe, respectively. The analysis accuracy was 1–1.5 relative%.

X-ray powder diffraction study of the synthesized phases was performed on a Stoe IPDS-2T diffractometer (MoKα radiation, graphite monochromator) using Gandolfi mode. Two-dimensional X-ray patterns were radially integrated using the X-Area software package. The diffraction profiles were treated using the WinXPow (Stoe) program packages. For the phase analysis, the database of PDF-4 Minerals [20] was used. Pyrites and plates of noble metals were analyzed from the surface.

3. Results

Table 1 shows the results of analysis of the composition of phases formed at the contact of pyrite and Au-Ag alloys of varying composition (No. 1–5). In the experiment with the starting composition Au + FeS_2 (No. 1), in which gold plates were used, newly formed phases are absent. However, detailed analysis showed the presence of fine-dispersed gold particles no more than 2 μm on the surface of pyrite blocks (Fig. 2a). In the experiment with the starting composition Ag + FeS_2 (No. 5), the silver plates both in contact and out of contact with pyrite were completely replaced by acanthite. Fine- and coarse-grained aggregates of spear-shaped and box-line crystals of silver sulphide formed on the silver plate that was out of contact with pyrite (Fig. 3a–c). Near the contact with the silver plate on the surface of pyrite and in the cracks pyrrhotite and acanthite formed (Fig. 4a–d). Fig. 4d shows the overgrowth of pyrite with crystals of pyrrhotite and acanthite.

The same as in the experiment with metal silver (Table 1, No. 5), in the experiments with Au-Ag alloys (Table 1, No. 2–4), pyrrhotite formed only on the surface of pyrite near the metal plates. Fig. 5. shows the distribution of phases in the reaction zones with Au-Ag alloys of initial compositions $Au_{0.56}Ag_{0.44}$ (a), $Au_{0.35}Ag_{0.65}$ (b) and $Au_{0.19}Ag_{0.81}$ (c). It is well seen that pyrite zone is replaced by pyrrhotite with rare microinclusions of Au-Ag sulphides in the intergrain space, further lies the zone of Au-Ag sulphides containing the inclusions of Au-Ag alloys. Au-Ag sulphides – acanthite and uytenbogaardtite – form intergrowths that are similar to decay structures. They differ in the shades of gray color: light phase in the form of thin veinlets is uytenbogaardtite, and the main dark phase is acanthite. The compositions of acanthite and uytenbogaardtite are unstable and widely vary in Au, Ag and S (Table 1, No. 2–4). In all experiments, deficit of gold in uytenbogaardtite compared to its stoichiometric composition was observed. This may be related to the small sizes of this phase and its intergrowth with acanthite, which leads to the overestimation of silver quantity in the composition of uytenbogaardtite in microprobe analysis.

The compositions of pyrrhotites and newly formed Au-Ag alloys differ in experiments No. 2–4 (Table 1). The composition of pyrrhotite with the maximum iron content $Fe_{0.873 \pm 0.002}S$ was established in the experiment with the starting alloy of composition $Au_{0.56}Ag_{0.44}$ (No. 2, Table 1), whereas the composition of pyrrhotite with the minimum iron content $Fe_{0.860 \pm 0.002}S$ was found in the experiment with the starting alloy of composition $Au_{0.35}Ag_{0.65}$ (No. 3, Table 1). Similar concentrations of Fe in pyrrhotite $Fe_{0.866 \pm 0.002}S$ and $Fe_{0.867 \pm 0.002}S$ within analytical error were found in experiments No. 4 and 5, in which the starting alloy was of composition $Au_{0.19}Ag_{0.81}$ and Ag.

It is worth noting that the Au-Ag plates located out and in contact with pyrite in the experiments with Au-Ag alloys of starting compositions $Au_{0.56}Ag_{0.44}$, $Au_{0.35}Ag_{0.65}$ and $Au_{0.19}Ag_{0.81}$ (Table 1, No. 2–4) are completely replaced and have similar compositions of newly formed Au-Ag alloys and Au-Ag sulphides.

The maximum change in the compositions of alloys (Au_Δ = 0.3 mol fraction) was detected in the experiment in which the starting alloy of $Au_{0.19}Ag_{0.81}$ was replaced by the alloy of $Au_{0.49}Ag_{0.51}$ (No. 4, Table 1). The minimum change in the compositions of alloys (Au_Δ = 0.05 mol fraction) was found in the experiment in which the starting of alloy $Au_{0.56}Ag_{0.44}$ increased to $Au_{0.61}Ag_{0.39}$ (No. 2, Table 1). The composition of alloy $Au_{0.35}Ag_{0.65}$ (No. 3) grew to $Au_{0.45}Ag_{0.55}$, i.e. by 0.1 mol fraction Au.

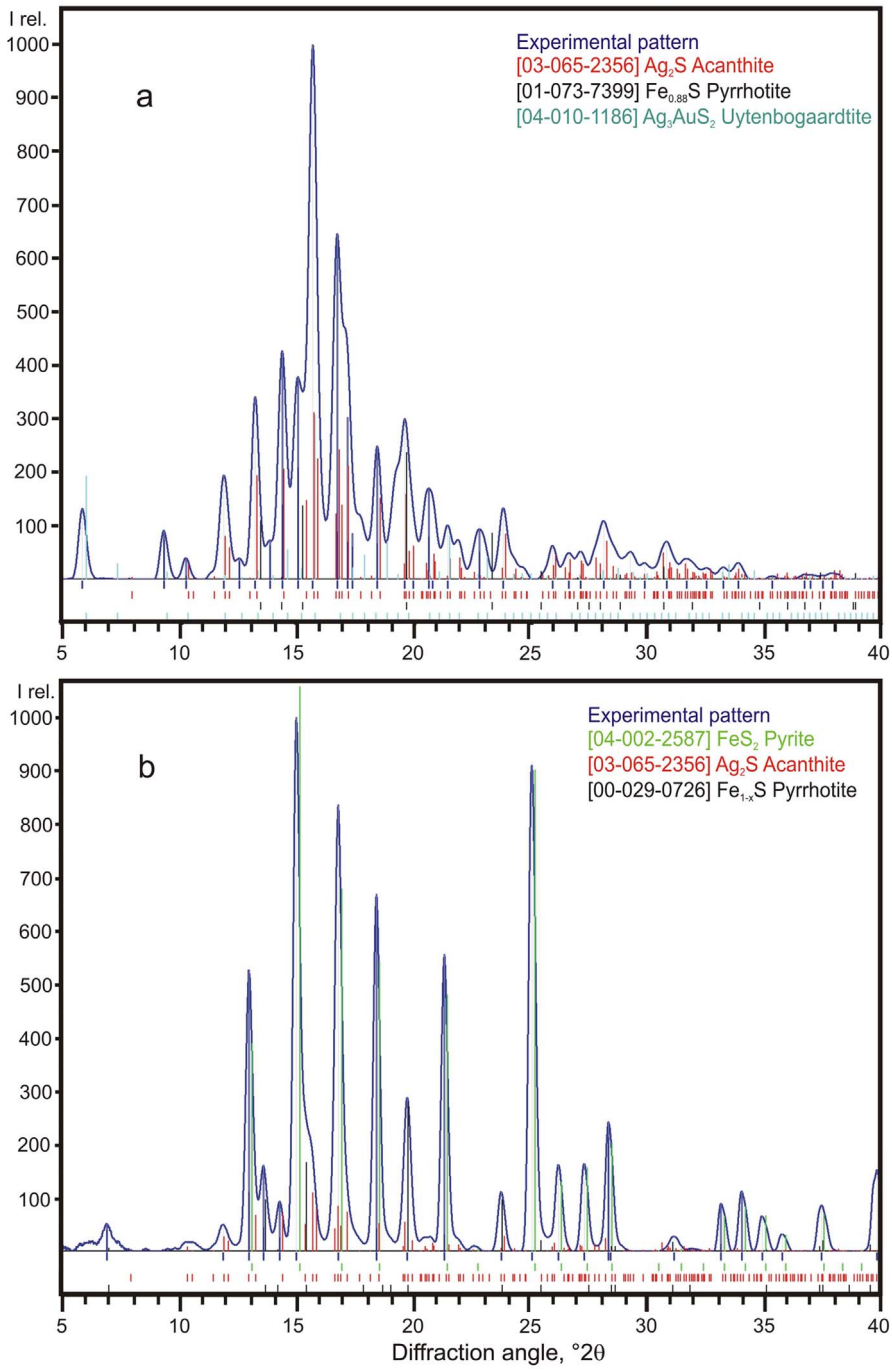

Fig. 6. X-ray powder diffraction pattern of sample No. 3 (a) and No. 5 (b) a with starting alloys of compositions $Au_{0.56}Ag_{0.44}$ and Ag in accordance. Vertical lines under graph represent the positions of peaks (from top to bottom): Experimental pattern, uytenbogaardtite Ag_3AuS_2, pyrrhotites $Fe_{0.88}S$ and $Fe_{1-x}S$, acanthite Ag_2S and residual pyrite FeS_2. The bottom of the figure shows a bar chart for each phase in the same sequence as in the phase at the top of the list on the right.

The XRD data show the absence of pyrrhotites and newly formed phases in the solid-phase products of experiment No. 1 (Au + FeS_2) (Table 1). Samples No. 2–4 contains acanthite (PDF card 03-065-2356), uytenbogaardtite (04-010-1186) and pyrrhotite $Fe_{0.88}S$ (01-073-7399) or $Fe_{1-x}S$ (00-029-0726). Fig. 6a shows the diffraction pattern of solid-phase products of the experiment with Au-Ag alloy of compositions $Au_{0.56}Ag_{0.44}$ (No. 3, Table 1). The ratio of the intensities of the peaks of Au-Ag sulphides shows that the concentration of uytenbogaardtite is considerably lower than that of acanthite. Sample No. 5 (Ag + FeS_2) contain acanthite (03-065-2356), pyrrhotite $Fe_{1-x}S$ (00-029-0726) and residual pyrite (Fig. 6b).

Magnetic phases in the experimental solid-phase products have not been detected. In accordance with the Fe-S diagrams [21,22], hexagonal nonmagnetic pyrrhotite is stable at 450 °C. The data from [23,24] evidence that pyrrhotite ($Fe_{1-y}S$) may be monoclinic or hexagonal. However, the presence of other highly concentrated phases in the samples made it impossible to establish the modification of pyrrhotite from the data of diffraction experiment.

4. Discussion

The results obtained evidence that desulphidation of pyrite with formation of pyrrhotite took place only in the experiments with Au-Ag alloys and metallic silver (Table 1, No. 2–5). In the experiment with

starting composition Au + FeS_2 (Table 1, No. 1), pyrrhotite was not found either in pyrite or on its surface. Microparticles of gold (Fig. 2a) found of the surface of pyrite in this experiment, most likely, formed from the gas phase which resulted from heating and annealing of starting substances. These data suggest that the presence of gold in the system makes pyrite more stable, probably owing to the appearance fine-dispersed particles on its surface, which prevent formation of pyrrhotite.

According to the method of solid-phase diffusion [19] used in the experiments, a reaction process is considered to be completed and the system is close to equilibrium if one of the starting components is consumed. In the experiments No. 2–5 there were no residue of initial metal plates. The starting plates No. 2–4 both in contact and out of contact with pyrite were fully replaced by acanthite, uytenbogaardtite and Au-Ag alloys with higher content of Au. In case of silver (No. 5), it was completely transformed into acanthite (see Table 1). Thus, it may be concluded that chemical reactions in these experiments are completed and have reached equilibrium conditions.

Variations in the compositions of pyrrhotites (No. 2–5) and Au-Ag alloys (No. 2–4) in different experiments (Table 1) are totally regular, as the experiments were conducted in the ampoules isolated from each other and, hence, sulphur fugacity (fS_2) varied. Under experimental conditions fS_2 was determined by temperature, pyrite-pyrrhotite buffer and activity of silver and gold in starting alloys.

The pyrrhotite composition was determined by the equation from [25]:

$$x = 1.45 \cdot 10^{-4} \cdot (t + 273.15) + 1.035, \quad (1)$$

where x – mol fraction in FeS_x and t – the temperature over the range of 347–700 °C, for the reaction of thermal decomposition of pyrite in vacuum:

$$FeS_2\ (s) \leftrightarrow FeS_x\ (s) + 0.5 \cdot (2\text{-}x)\ S_2\ (g), \text{ where } 1 < x < 1.23, \quad (2)$$

at 450 °C x is 1.1403. Data of microprobe analysis show that the contents of S in pyrrhotite in terms of one molar fraction of iron in experiments No. 2–5 (Table 1) are somewhat higher and amount to 1.145–1.163. Deviations in pyrrhotite composition might be due to the varying activity of gold and silver in the alloy, which influences sulphur fugacity in the experiments.

The obtained results on the annealing of pyrite out and in contact with Au-Ag alloys at 450 °C show that the amount of uytenbogaardtite is considerably lower than that of acanthite. Petrovskaite, which is the Au-richest gold and silver sulphide, was not found in the solid-phase products of the experiments. Its absence may be related to the lack of high sulphur fugacity under experimental conditions.

The formation of Au-Ag sulphides in the presence of pyrite, most likely, takes place under the interaction of gaseous sulphur with noble metals rather than solid phase reactions as was assumed previously in the experiments on thermal diffusion [17]. Sulphidation of Ag and Au-Ag plates, which were out of contact with pyrite in our experiments and in the experiments of other researchers [26–28], supports the participation of gaseous sulphur in sulphidation and desulphidation reactions. The mechanism of deposition of gold on pyrite with participation of gases has been discussed in many works [29–32]. The results obtained also prove the probable participation of gaseous forms of gold and sulphur in ore formation.

Under the metamorphism of pyrite and pyritic ores [32,33] the formation of Au-Ag sulphides is probable in the presence of native silver, kustelite or electrum. High-fineness and pure gold is resistant and no susceptible to sulphidation.

5. Conclusions

The presence of Ag promotes the transformation of pyrite into pyrrhotite and sulphidation and ennobling of Au-Ag alloys. Gold, on the contrary, stabilizes the resistance of pyrite and prevents its transformation into pyrrhotite. On heating, gold passes into a gas phase and is accumulated on the surface of pyrite. We predict the presence of Au-Ag sulphides, mainly acanthite, and smaller amounts of uytenbogaardtite in pyrite-bearing ores of metamorphic genesis, which contain native silver, kustelite or electrum. In gold-sulphide ores with high-fineness gold, these are absent.

Acknowledgments

This work is supported by the Russian Foundation for Basic Research (grant no. 14-05-00504a) and state assignment project (No. 0330-2016-0001). We thank N.S. Karmanov (Analytical Center for Multielemental and Isotope Research, Novosibirsk, Russia) for the electron microprobe studies of polished sections.

References

[1] R.W. Boyle, The Geochemistry of Silver and Its Deposits, Geological Survey of Canada, Ottawa, 1968.
[2] R.W. Boyle, The Geochemistry of Gold and Its Deposits, Geological Survey of Canada, Ottawa, 1979.
[3] A.F. Korobeinikov, V.A. Narseev, A.Y. Pshenichkin, P.S. Revyakin, Ch. Kh. Arifulov, Pyrites of Gold Deposits (Properties, Zoning, and Practical Application), TsNIGRI, Moscow, 1993. (in Russian).
[4] J. Zhou, B. Jago, C. Martin, Establishing the process mineralogy of gold ores, SGS Miner. Tech. Bull. 3 (2004) 1–16.
[5] J.P. Vaughan, The process mineralogy of gold: the classification of ore types, JOM 56 (2004) 46–48.
[6] I.V. Vikentyev, Invisible and microscopic gold in pyrite: methods and new data for massive sulfide ores of the Urals, Geol. Ore Deposits 57 (2015) 237–265.
[7] M.A.H. Altigani, R.K.W. Merkle, R.D. Dixon, Geochemical identification of episodes of gold mineralisation in the Barberton Greenstone Belt South Africa, Ore Geol. Rev. 75 (2016) 186–205.
[8] H.A. Cocker, J.L. Mauk, S.D.C. Rabone, The origin of Ag-Au-S-Se minerals in adularia-sericite epithermal deposits: constraints from the Broken Hills deposit Hauraki Goldfield, New Zealand, Miner. Deposita 48 (2013) 249–266.
[9] G.A. Palyanova, N.E. Savva, T.V. Zhuravkova, E.E. Kolova, Gold and silver minerals in low-sulfide ores of the Dzhulietta deposit (northeastern Russia), Russ. Geol. Geophys. 57 (2016) 1171–1190.
[10] C.P. Vidal, D.M. Guido, S.M. Jovic, R.J. Bodnar, D. Moncada, J.C. Melgarejo, W. Hames, The Marianas-San Marcos vein system: characteristics of a shallow low sulfidation epithermal Au-Ag deposit in the Cerro Negro district, Deseado Massif, Patagonia, Argentina, Miner. Deposita 51 (2016) 725–748.
[11] G. Palyanova, N. Karmanov, N. Savva, Sulfidation of native gold, Am. Mineral. 99 (2014) 1095–1103.
[12] G.A. Palyanova, K.A. Kokh, Yu.V. Seryotkin, Formation of gold-silver sulfides and native gold in Fe-Ag-Au-S system, Russ. Geol. Geophys. 53 (2012) 321–329.
[13] G. Pal'yanova, Yu. Mikhlin, K. Kokh, N. Karmanov, Yu. Seryotkin, Experimental constraints on gold and silver solubility in iron sulfides, J. Alloy. Compd. 649 (2015) 67–75.
[14] N.E. Savva, G.A. Pal'yanova, Genesis of gold and silver sulphides at the Ulakhan deposit (northeastern Russia), Russ. Geol. Geophys. 48 (2007) 799–810.
[15] N.E. Savva, G.A. Pal'yanova, M.A. Byankin, The problem of genesis of gold and silver sulfides and selenides in the Kupol deposit (Chukot Peninsula, Russia), Russ. Geol. Geophys. 53 (2012) 457–466.
[16] G.A. Pal'yanova, N.E. Savva, Specific genesis of gold and silver sulfides at the Yunoe deposit (Magadan Region, Russia), Russ. Geol. Geophys. 50 (2009) 587–602.
[17] G. Palyanova, K. Kokh, Yu. Seryotkin, Transformation of pyrite to pyrrhotite in the presence of Au-Ag alloys at 500 °C, Am. Mineral. 101 (2016) 2731–2737.
[18] V.F. Proskurnin, G.A. Palyanova, N.S. Karmanov, A.A. Bagaeva, A.V. Gavrish, B.S. Petrushkov, The first discovery of uytenbogaardtite in Taimyr (Konechnoe ore occurrence), Dokl. Earth Sci. 441 (2011) 1661–1665.
[19] Z. Jin, A study of the range of stability of phase in some ternary systems, Scand. J. Metall. 10 (1981) 279–287.
[20] The Powder Diffraction File PDF-4+, International Centre for Diffraction Data (ICDD), Release, 2006.
[21] G. Kullerud, H.S. Yoder, Pyrite stability relations in the Fe-S system, Econ. Geol. 54 (1959) 533–572.
[22] R.G. Arnold, Equilibrium relations between pyrrhotite and pyrite from 325° to 741 °C, Econ. Geol. 57 (1962) 72–90.
[23] H. Wang, I. Salveson, A review on the mineral chemistry of the non-stoichiometric iron sulphide, $Fe_{1-x}S$ ($0 \le x \le 0.125$): polymorphs, phase relations and transitions, electronic and magnetic structures, Phase Transitions 78 (2005) 547–567.
[24] D.A. Chareev, E.G. Osadchii, Thermodynamic studies of pyrrhotite–pyrite equilibria in the Ag–Fe–S system by solid-state galvanic cell technique at 518–723 K and total pressure of 1 atm, Geochim. Cosmochim. Acta 70 (2006) 5617–5633.
[25] J.M. Lambert, J.R. Simkovich, P.L. Walker, The kinetics and mechanism of the pyrite-to-pyrrhotite transformation, Metall. Trans. B 29B (1998) 385–396.
[26] P.B. Barton Jr., P. Toulmin, The electrum-tarnish method for the determination of

the fugacity of sulfur in laboratory sulfide systems, Geochim. Cosmochim. Acta 28 (1964) 619–640.
[27] P. Toulmin, P.B. Jr. Barton, A thermodynamic study of pyrite and pyrrhotite, Geochim. Cosmochim. Acta 28 (1964) 641–671.
[28] D.M. Francis, Electrum-Tarnish by Sulfur: a Study of an Irreversible Processes. A Thesis of Degree Master of Science, The University of British Columbia, 1971.
[29] S. Scher, A.E. Williams-Jones, G. Williams-Jones, Fumarolic activity acid-sulfate alteration, and high sulfidation epithermal precious metal mineralization in the crater of Kawah Ijen volcano, Java, Indonesia, Econ. Geol. 108 (2013) 1099–1118.
[30] G.S. Pokrovski, N.N. Akinfiev, A.Y. Borisova, A.V. Zotov, K. Kouzmanov, Gold speciation and transport in geological fluids: insights from experiments and physical-chemical modelling, in: P.S. Garofalo, J.R. Ridley (Eds.), Gold-Transporting Hydrothermal Fluids in the Earth's Crust, Geological Society, London, 2014Special Publications 402 http://dx.doi.org/10.1144/SP402.4.
[31] G.S. Pokrovski, A.Y. Borisova, A.Y. Bychkov, Speciation and transport of metals and metalloids in geological vapors, Rev. Mineral. Geochem. 76 (2013) 165–218.
[32] A.G. Tomkins, Windows of metamorphic sulfur liberation in the crust: implications for gold deposit genesis, Geochim. Cosmochim. Acta 74 (2010) 3246–3259.
[33] J.R. Craig, F.M. Vokes, The metamorphism of pyrite and pyritic ores: an overview, Mineral. Mag. 57 (1993) 3–18.